BMC Genomics

RESEARCH

Open Access

Identification and characterization of the tumor necrosis factor receptor superfamily in the Chinese tree shrew (*Tupaia belangeri chinensis*)

Zongjian Huang[1,2†], Nan Shi[1,2†], Zhenqiu Luo[1,2], Fangfang Chen[1,2], Xunwei Feng[1,2], Yongjing Lai[1,2], Jian Li[1,2], Xiang Yi[1,2], Wei Xia[1,2*] and Anzhou Tang[1,2,3*]

Abstract

The tumor necrosis factor receptor superfamily (TNFRSF) plays a vital role in eliciting immune responses against infections. The tree shrew, closely related to primates, is often utilized in human disease models. Here, we analyzed TNFRSF members from 11 different animal species, including the Chinese tree shrew, and identified 24 tree shrew TNFRSF (tTNFRSF) genes, which were grouped into seven subcategories with similar motifs, sequences, and gene structures. As expected, the multi-species collinearity analysis revealed that tTNFRSF genome bears a greater resemblance to humans than to mice. Transcriptome data from 28 samples across ten organ types showed high TNFRSF expression predominantly in immune organs. It was seen that TNFRSF13C co-expresses consistently with the B cell surface marker CD79A, which is consistent with its characteristics in humans. The tissue distribution and co-expression were confirmed via RT-qPCR and immunofluorescence. Evaluation of transcriptome data from 70 samples infected with six types of viruses showed that most TNFRSF genes were upregulated in tree shrew post-viral infection. TNFRSF exerts antiviral function most probably through the activation of the NF-κB pathway, subsequently causing apoptosis of infected cells. Our findings provide evolutionary and functional insights into tTNFRSF, indicating its potential utility in human viral infection models.

Keywords TNFRSF, Tree shrew, Innate immunity, Viral infection, Animal model

†Zongjian Huang and Nan Shi contributed equally to this work.

*Correspondence:
Wei Xia
YFY004532@sr.gxmu.edu.cn
Anzhou Tang
tanganzhou@gxmu.edu.cn
[1]Department of Otorhinolaryngology Head and Neck Surgery, The First Affiliated Hospital of Guangxi Medical University, Nanning, Guangxi 530000, China
[2]Key Laboratory of Early Prevention and Treatment for Regional High Frequency Tumors (Guangxi Medical University), Ministry of Education, Nanning, Guangxi 530000, China
[3]State Key Laboratory of Targeting Oncology, Guangxi Medical University, Nanning, Guangxi 530021, China

Introduction

The tree shrew is routinely used in human disease model studies owing to its several advantageous features such as a small size, brief reproductive cycle, and low upkeep cost [1, 2]. However, one of its most significant characteristics is that it exhibits a higher genetic affinity to humans than conventional laboratory animals such as rats, mice, and rabbits [3–6]. Recent studies have unveiled the fundamental physiological attributes of tree shrews [7–13]. The cytokines and chemokines found in tree shrews are likely to have functions analogous to those in humans [14]. Additionally, the polysaccharide-immune serum of tree shrews can induce antibody-dependent antimicrobial reactions, resembling human immune processes [15]. This makes tree shrews particularly suitable for research on human infectious diseases. They are currently used in various viral infection model studies, including those for Epstein-Barr virus (EBV), hepatitis B and C virus (HBV, HCV), herpes simplex virus (HSV), Zika virus, dengue virus, and influenza virus [16–25]. With successful breeding and subsequent establishment of transgenic tree shrews [26, 27], their use in biomedical research is expected to increase. Thus, understanding the immune system of tree shrews, particularly the genes related to pathogenic infection and surveillance, is crucial for gaining insights into their immune responses, molecular biological processes, and the clinical applicability of related research.

When a virus enters the body, a series of complex immune responses is rapidly initiated to combat the intrusion of the pathogen. This system integrates both innate and adaptive immunity along with precise cytokine regulation, presenting a comprehensive defense strategy against viral invasion. The deployment and activation of various cytokines, including tumor necrosis factor (TNF), interferons, interleukins, chemokines, and colony-stimulating factors, are integral to the body's resilience against viral infections. TNF is a major proinflammatory cytokine that regulates the activity of immune cells and stimulates inflammatory responses during viral infection. The tumor necrosis factor receptor superfamily (TNFRSF) is an essential cell-surface cytokine receptor group that plays a critical role in cell differentiation, facilitation of host immune defense, mediation of inflammatory responses, and signal transduction [28]. A total of 29 TNFRSF members have been characterized within the human genome, which are primarily classified as type I transmembrane proteins. The principal structural components of this receptor family include extracellular, transmembrane, and intracellular domains, which recruit signal transduction proteins [29]. The characteristic domain of TNFRSF is the cysteine-rich domain (CRD) within the extracellular domain and is the main region where TNFRSF receptors bind to ligands [30]. Some members also possess a characteristic death domain (DD), which is fundamental for activating the classical cellular apoptosis signaling pathway [31, 32]. Apart from this, TNFRSF is involved in activating the signaling pathways of transcription factors such as NF-κB and JNK, thereby contributing to immune regulation and cellular apoptosis [33–35].

TNFRSF plays a dual role in the host immune system's fight against viral infections. Following viral infection, host immune cells can initiate apoptosis related to a TNF receptor to limit viral replication and expose it to the humoral immune response [36, 37]. Conversely, viruses that endure robust host immune eradication pressure continuously adapt and evolve, fostering diverse mechanisms to suppress the immune system. For instance, some viruses can encode viral TNF receptors (vTNFRs), which share a similar structure and function with host TNFRSF receptors [38]. These vTNFRs can thus competitively block the mutual recognition and interaction between TNFRSF receptors and ligands, inhibiting the activation of the apoptosis signaling pathway. For instance, the LMP1 protein of EBV shares structural and functional similarities with TNFRSF5 and is capable of preventing TNFRSF5 (also known as CD40) from activating the CD40 pathway. This inhibits the transformation of activated B cells into plasma cells, thereby aiding EBV in evading immune surveillance [39, 40].

An in-depth analysis of the molecular characteristics and functions of TNFRSF members can enhance our understanding of the immune response processes in tree shrews. This knowledge can advance the research on tree shrew animal models and facilitate antiviral drug development based on these models. Thus, the present study aimed to characterize the structure, physiochemical properties, and functions of the TNFRSF members in the Chinese tree shrew (*Tupaia belangeri chinensis*). We identified 24 tree shrew TNFRSF (tTNFRSF) genes, which were categorized into seven phylogenetic subgroups. Furthermore, this study incorporated transcriptome sequencing data from various virus-infected tree shrew models to investigate the expression alterations and functional mechanisms of TNFRSF prompted by viral infection.

Materials and methods

Animals

Healthy adult tree shrews ($n = 9$) were purchased from the Experimental Animal Center of the Kunming Institute of Zoology, Chinese Academy of Sciences. The animals were anesthetized with pentobarbital sodium solution, and tissues (spleen, tonsils, lymph nodes, and thymus) were obtained from three animals. The tissues were either rapidly frozen in liquid nitrogen and stored at − 80 °C or fixed in 10% neutral formalin, embedded in

paraffin, and sectioned. Peripheral blood was collected for the extraction of peripheral blood mononuclear cells (PBMCs), which were separated from whole blood by Ficoll gradient centrifugation (Solarbio, Beijing, China).

Viral inoculation

EBV suspension was prepared as previously described [16]. The tree shrews ($n=6$) were injected intravenously with EBV suspension containing 1×10^8 copies, and on the 7th and 28th day post-inoculation, the tree shrews were euthanized. Peripheral blood samples were collected for PBMC extraction and other samples were preserved for further experiments.

Phylogenetic analysis of TNFRSF genes from 11 species

The amino acid and gene sequences of TNFRSF genes from *Tupaia belangeri chinensis* (Chinese tree shrew) and 10 other mammalian species (*Homo sapiens*, *Mus musculus*, *Rattus norvegicus*, *Macaca mulatta*, *Gorilla gorilla*, *Ovis aries*, *Bos taurus*, *Sus scrofa*, *Oryctolagus cuniculus*, and *Canis lupus familiaris*) were obtained from the NCBI database (https://www.ncbi.nlm.nih.gov/gene). Details can be found in Table S1.

Multiple sequence alignment of TNFRSF genes from these 11 species—tree shrew, human, mouse, rat, rhesus monkey, gorilla, sheep, cattle, pig, rabbit, and dog—was conducted using the MUSCLE algorithm implemented in the MEGA-11 software [41]. The algorithm used was the neighbor-joining (NJ) model, the validated bootstrap value was set to 1000, and the model selection parameter was Poisson. The classification is based on the similarity of gene sequences and evolutionary relationships.

Analysis of TNFRSF gene structure, conserved motifs and domains, and physicochemical properties

The structure of TNFRSF genes in tree shrew was predicted and analyzed using Tbtools-II v2.088 [42]. The conserved domains and motifs of the 24 tTNFRSF genes were predicted using the MEME online system (http://memesuite.org/tools/meme/) and the number of motifs was set to 8. The conserved domains were predicted using the conserved domain database of NCBI (https://www.ncbi.nlm.nih.gov/Structure/bwrpsb/bwrpsb.cgi). A hydropathy plot was generated using online analysis tools (http://web.expasy.org/protscale, http://web.expasy.org/protparam) to predict the physicochemical properties of the amino acid sequences, including the molecular formula, total number of atoms, molecular weight, theoretical isoelectric point (pI), instability index (II), and grand average of hydropathicity of the proteins.

Chromosomal localization and collinearity analysis of TNFRSF genes in tree shrew

The chromosomal distribution of the tTNFRSF gene family across 30 autosomal chromosomes of the tree shrew, excluding sex chromosomes, was mapped using the positional annotation data from the GFF file of the tree shrew genome (KIZ version 3 database: http://www.treeshrewdb.org/index.html). The genome and annotation files of Homo sapiens (GRCh38) and Mus musculus (GRCm39) versions were downloaded from the Ensembl database (https://useast.ensembl.org/Homo_sapiens/Info/Index, https://useast.ensembl.org/Mus_musculus/Info/Index). The chromosomal location information of tTNFRSF genes was visualized using the Advanced Circos feature in TBtools-II v2.088. Intraspecific duplication events of tree shrew TNFRSF genes and interspecific collinearity analysis between tree shrew, human, and mouse genomes were performed using the MCScanX tool in TBtools-II v2.088, with the e-value set to 1×10^{-3}. The results were visualized using TBtools software, and the Multiple Synteny Plot tool highlighted the segmental duplication events of tTNFRSF genes. To further assess the selection pressure on TNFRSF collinear gene pairs, we extracted CDS sequences of TNFRSF genes and aligned them using MUSCLE, a tool available within MEGA11 software. The alignment results were then analyzed using KaKs_Calculator 2.0 to calculate the non-synonymous mutation rate (Ka), synonymous mutation rate (Ks) and the Ka/Ks ratio (nonsynonymous/synonymous) for each TNFRSF collinear gene pair [43].

RNA extraction and gene expression analysis

Total RNA was extracted from tree shrew tissues and their peripheral blood PBMCs using the RNeasy Plus Mini Kit (Qiagen, Germany), following the manufacturer's instructions. The RNA was reverse transcribed into cDNA using the PrimeScript™ RT reagent Kit with gDNA Eraser (TaKaRa, Dalian, China). RT-qPCR was performed using a Bio-Rad CFX 96 detection system and TB Green Premix Ex Taq (TaKaRa, Dalian, China). Specific quantitative primers for the TNFRSF genes are listed in Table S2 (reaction conditions followed the manufacturer's instructions). GAPDH was used as a reference gene for quantitative RT-PCR. The relative cycle threshold (CT) of each was averaged across the technical replicates. The resulting CT value of each gene was normalized to the geometric mean of the CT value of the reference gene (GAPDH) by subtracting the mean CT of the reference gene from the CT value of the gene ($2-\Delta CT$ method). Each experiment was repeated thrice.

RNA sequencing

RNA extraction, library construction, and sequencing protocols were provided by Beijing Novogene

Bioinformatics Technology Co., Ltd. The raw data obtained after sequencing underwent filtering, sequencing error rate check, and GC content distribution check to acquire clean reads for subsequent analyses. The quality-controlled clean reads were aligned to the tree shrew reference genome (http://www.treeshrewdb.org/) using the HISAT2 software (v2.2.1). Sequences with a similarity < 0.9 and coverage < 0.85 were filtered out to eliminate redundant sequences in the alignment results. The featureCounts (1.5.0-p3) tool was employed to calculate the read counts mapped to each gene and compute the fragments per kilobase of transcript per million mapped reads for each gene. We constructed a protein-protein interaction (PPI) network for tree shrew TNFRSF utilizing the STRING online database (http://string-db.org/). To identify key regulatory genes, differential gene PPI networks were calculated using the Stress and DMNC algorithms in the cytoHubba plugin of Cytoscape.

Immunofluorescence detection of target protein expression in tree shrew spleen

Immunofluorescence was performed on 4 μm sections of tree shrew spleen tissue. A TSA Immunofluorescence Kit (RS0036, ImmunoWay, USA) was used following the manufacturer's instructions. After dewaxing, antigen retrieval was performed in Tris-EDTA buffer (pH 9) under high pressure. Subsequently, endogenous peroxidase activity was blocked by incubating the sections in a 0.5% H_2O_2 solution for 15 min. The sections were then incubated overnight with a primary antibody (TNFRSF13C, 1:200, Abcam, ab33901), followed by a 30-min incubation at room temperature with a secondary antibody, and incubation with TSA-488 dye for 10 min. The sections were then heated in a preheated antibody removal solution for 15 min and incubated overnight with a primary antibody (CD79A, 1:100, Santa Cruz, sc-20064), followed by incubation with a secondary antibody and TSA-594 dye. DAPI was used for nuclear staining, and the sections were coverslipped using an anti-quenching mounting medium. Sections were observed, and images were captured using a fluorescence microscope (Eclipse Ci-L, Nikon, Japan).

Statistical analysis

Statistical analyses were performed using GraphPad Prism software version 9.0.0. Statistical significance between two groups was determined using t-tests. Comparisons among more than two groups were performed using ANOVA. A p-value < 0.05 was considered statistically significant.

Results

Analysis of alignment, phylogenetic relationship and classification of the TNFRSF genes

To understand the similarities and phylogenetic relationships of the TNFRSF members found in tree shrews, we compared 24 TNFRSF genes from tree shrew (*Tupaia belangeri chinensis*) to those from humans (29), rhesus monkeys (28), mice (27), gorillas (27), cattle (27), rats (25), sheep (25), pigs (25), dogs (24), and rabbits (22). All gene sequences were publicly accessible from the NCBI website. Multiple sequence alignment was performed for the TNFRSF genes of these 11 species with the 24 tTNFRSF genes as a reference. MEGA-11 was used to construct a neighbor-joining phylogenetic tree for the tTNFRSF genes (Fig. 1). Based on their evolutionary relationships, TNFRSF genes were divided into seven major clusters (I–VII) (Table S3). The phylogenetic tree revealed that 11 out of the 24 TNFRSF genes in tree shrews (TNFRSF3, 4, 6, 8, 10 A, 11 A, 11B, 13B, 13 C, 14, and 16) clustered more closely with those in humans and other primates compared to non-primate species. Specifically, 7 genes (TNFRSF1B, 7, 9, 12 A, 17, 19, 19 L) clustered with non-primate species, emphasizing the closer evolutionary relationship with primates. Thus, the function of TNFRSF genes in tree shrews is speculated to be closest to that of humans, particularly in their role in providing immunity and their mechanism of action with immune molecules.

Members within a tTNFRSF subgroup exhibited structural and motif similarity

The conserved motifs and domains of tTNFRSF proteins were identified using the MEME software (Fig. 2). Motif prediction analysis revealed eight distinct motifs, designated as motifs 1–8. Table S4 provides details of the length and sequence data for each motif. The number of motifs in each TNFRSF protein ranged from 1 to 7, with all genes, except TNFRSF19 containing motif 8. Group I consistently contained motifs 6 and 8, whereas Group II contained motifs 1, 2, 3, 6, and 8. All genes in Group IV included motifs 2, 4, and 8, while those in Group V shared motif 8 and all genes in Group VII exhibited the presence of motif 5. Analysis of the conserved domains revealed that, except for TNFRSF13C, all genes possessed the TNFRSF domain. Genes in Group IV, along with TNFRSF6, TNFRSF11B, TNFRSF21, and EDAR, included the DD. However, TNFRSF13C exclusively featured a conserved domain of the BAFFR-TALL-BIND superfamily. In summary, members of the same tTNFRSF subgroup exhibited similar gene structures and motif compositions and tended to cluster together in the phylogenetic tree.

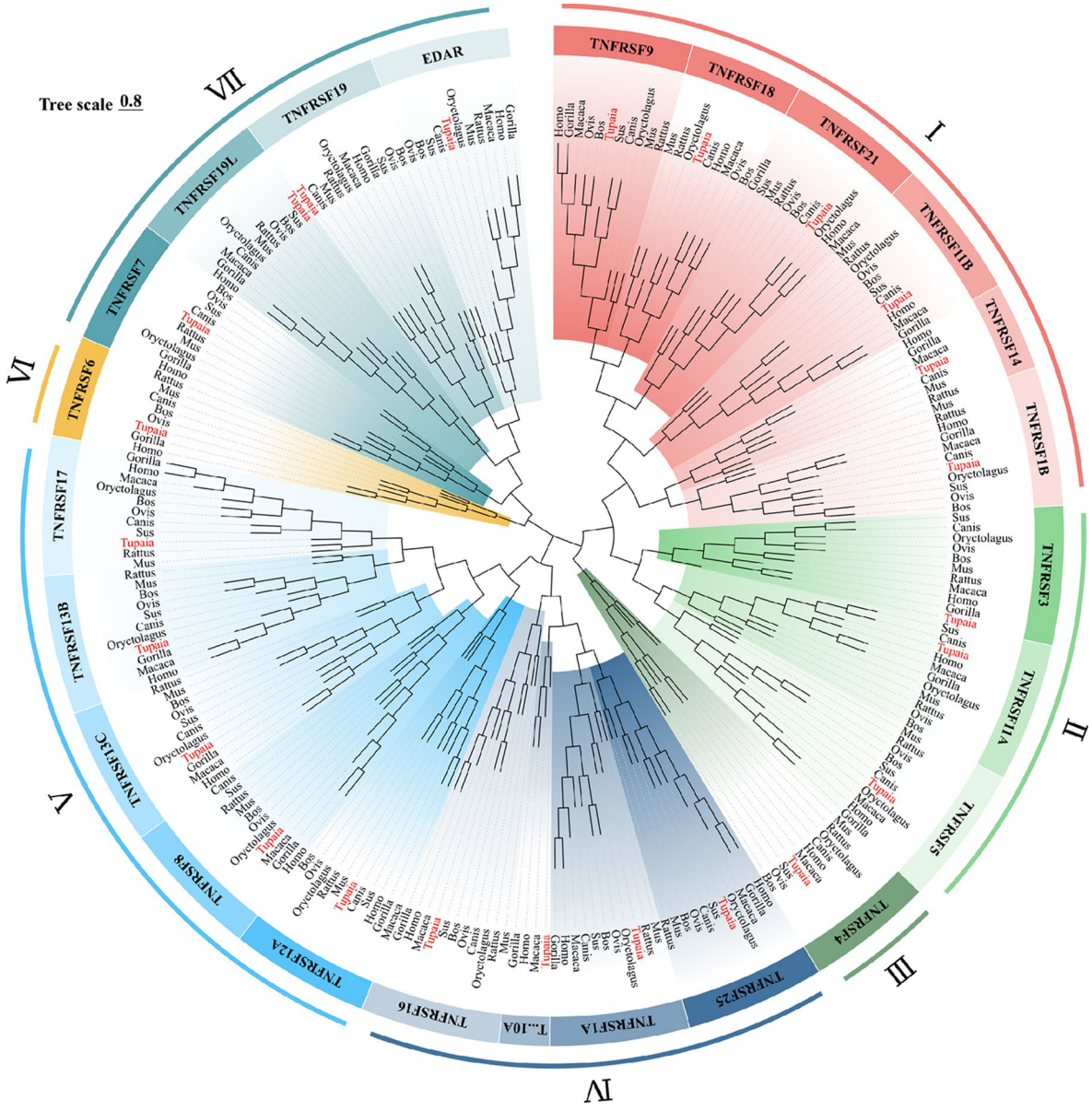

Fig. 1 Phylogenetic analysis of TNFRSF genes from 11 species. Using the MEGA-11 software, unrooted phylogenetic trees were constructed to compare tree shrew TNFRSF genes with homologous genes from *Homo sapiens*, *Mus musculus*, *Rattus norvegicus*, *Macaca mulatta*, *Gorilla gorilla*, *Ovis aries*, *Bos taurus*, *Sus scrofa*, *Oryctolagus cuniculus*, and *Canis lupus familiaris*. The tree was derived using the neighbor-joining (NJ) method with 1,000 bootstrap replicates and categorized the TNFRSF genes into 7 subclades (outer circles). Different colors have been used to represent the various TNFRSF genes, and genes from tree shrews are marked in red, while those from other species are marked in black. T…10 A, TNFRSF10A

Physicochemical properties of tTNFRSF proteins

We evaluated the physicochemical properties of tTNFRSF proteins to gain insight into their functions. Figure 3 and Table S5 present the hydrophobicity plots, molecular formula, total atom count, molecular weight, theoretical pI, instability index (II), and grand average of hydropathicity of tTNFRSF proteins. The predicted results classify tTNFRSF6 as a stable protein. Additionally, among all the tTNFRSF genes, tTNFRSF6 stood out for its high hydrophilicity, whereas tTNFRSF12A was the most hydrophobic. The average hydrophobicity scores of most tTNFRSF receptors were less than 0. Moreover, as shown in Fig. 3, each member of tTNFRSF contained regions with relatively high hydrophobicity. Analysis of their physicochemical properties suggests that these receptors likely possess a transmembrane structure and are predominantly located on the cell membrane.

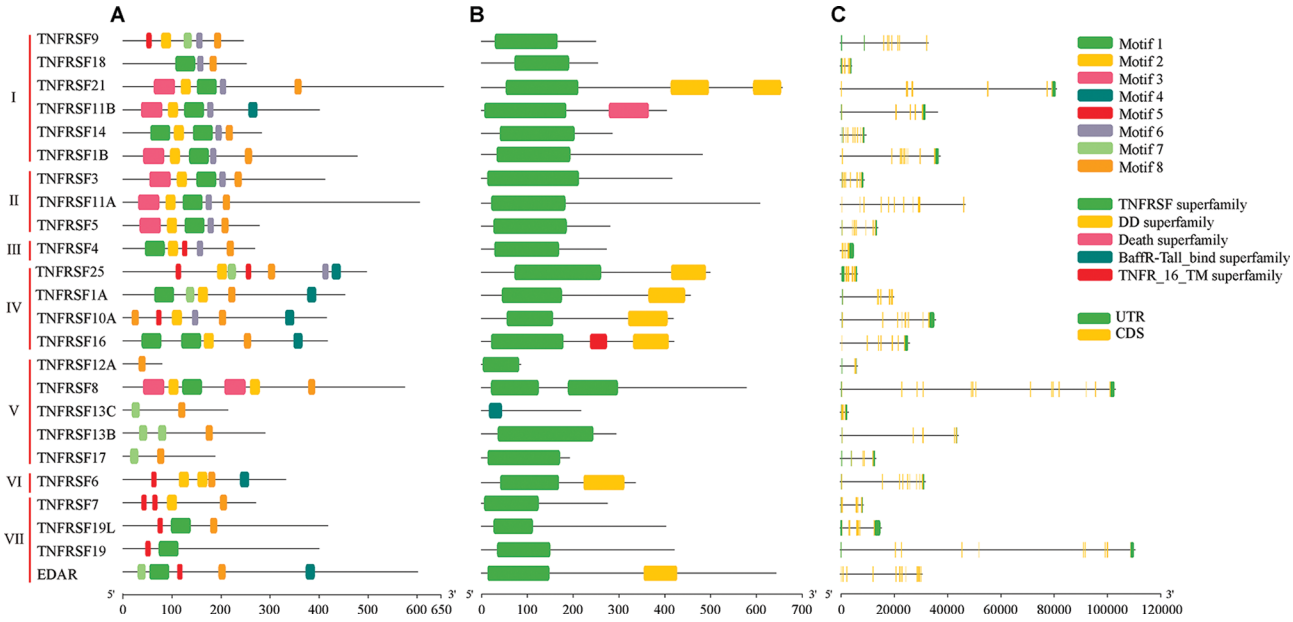

Fig. 2 Structural and motif similarity within TNFRSF subgroups. The MEME software was used to predict conserved motifs (**A**) and conserved domains (**B**) of TNFRSF proteins. The colored boxes represent different motifs and conserved domains. (**C**) Structure of tree shrew TNFRSF genes, where green boxes indicate non-coding regions, yellow boxes represent coding sequences (CDS), and black lines depict introns. The horizontal axis represents the length of the gene or amino acid sequence

TNFRSF genes are highly conserved and tree shrews are genetically closer to humans than to mice in terms of TNFRSF genes

Segmental duplication of tTNFRSF genes was further analyzed within the tree shrew genome. No tandem or segmental duplication events were observed in tTNFRSF genes. This suggests that tandem repeat events do not contribute to the expansion of tTNFRSF genes. The outer yellow squares in Fig. 4A represent 30 pairs of tree shrew chromosomes, with 24 TNFRSF genes unevenly distributed on 11 chromosomes. Chromosome 12 in tree shrew harbors eight TNFRSF genes, including TNFRSF1B, 4, 8, 9, 11 A, 14, 18, and 25, the highest number of TNFRSF gene members in tree shrews. As shown in Fig. 4B, there are 15 orthologous pairs of TNFRSF genes between tree shrews and humans (tTNFRSF and hTNFRSF) and 14 orthologous pairs between tree shrews and mice (tTNFRSF and mTNFRSF). This indicates a higher sequence similarity between tree shrews and humans than between tree shrews and mice at the TNFRSF gene level. Furthermore, TNFRSF13B is not an orthologous gene between mice, humans, and tree shrews. It is possible that in species more closely related to mice, orthologous genes of TNFRSF13B could be found.

Next, we calculated the Ka/Ks ratio for the 29 orthologous pairs of TNFRSF genes between tree shrews and humans/mice (tTNFRSF and hTNFRSF/mTNFRSF) (Table S6). The lowest Ka/Ks ratio was 0.069946 (tTNFRSF16 and hTNFRSF16), followed by 0.080885 (tTNFRSF11B and hTNFRSF11B) and 0.522894 (tTNFRSF18 and hTNFRSF18). Additionally, the average Ks values for the orthologous pairs between tree shrews and humans and between tree shrews and mice were 0.54575373 and 0.97348536, respectively. Considering the mammalian gene mutation rate of $1.1–1.9\times10^{-8}$ per year, our results imply that the divergence times for TNFRSF was approximately 18.191791 and 32.449512 million years ago for tree shrews and humans and for tree shrews and mice, respectively. This indicates that tree shrews are genetically closer to humans than to mice in terms of TNFRSF genes. Additionally, the Ka/Ks value for all orthologous gene pairs was less than 1, with most not exceeding 0.5. This suggests that TNFRSF genes may have undergone significant positive purifying selection, indicating a high level of conservation in these genes.

Expression profiles of tTNFRSF genes in various tree shrew tissues

To compare the baseline expression of TNFRSF family genes across different tree shrew tissues, transcriptome sequencing data from six organs, including the brain, lungs, small intestine, kidneys, liver, and spleen, were downloaded from publicly available datasets, totaling 24 samples. The expression levels of TNFRSF family genes in these organs were analyzed. The data sources and information are listed in Table S7. Additionally, given the close relationship between TNFRSF genes and host immunity, we collected transcriptome sequencing data from the spleen, lymph node, thymus, tonsils, and peripheral blood mononuclear cells (PBMCs) of healthy adult tree

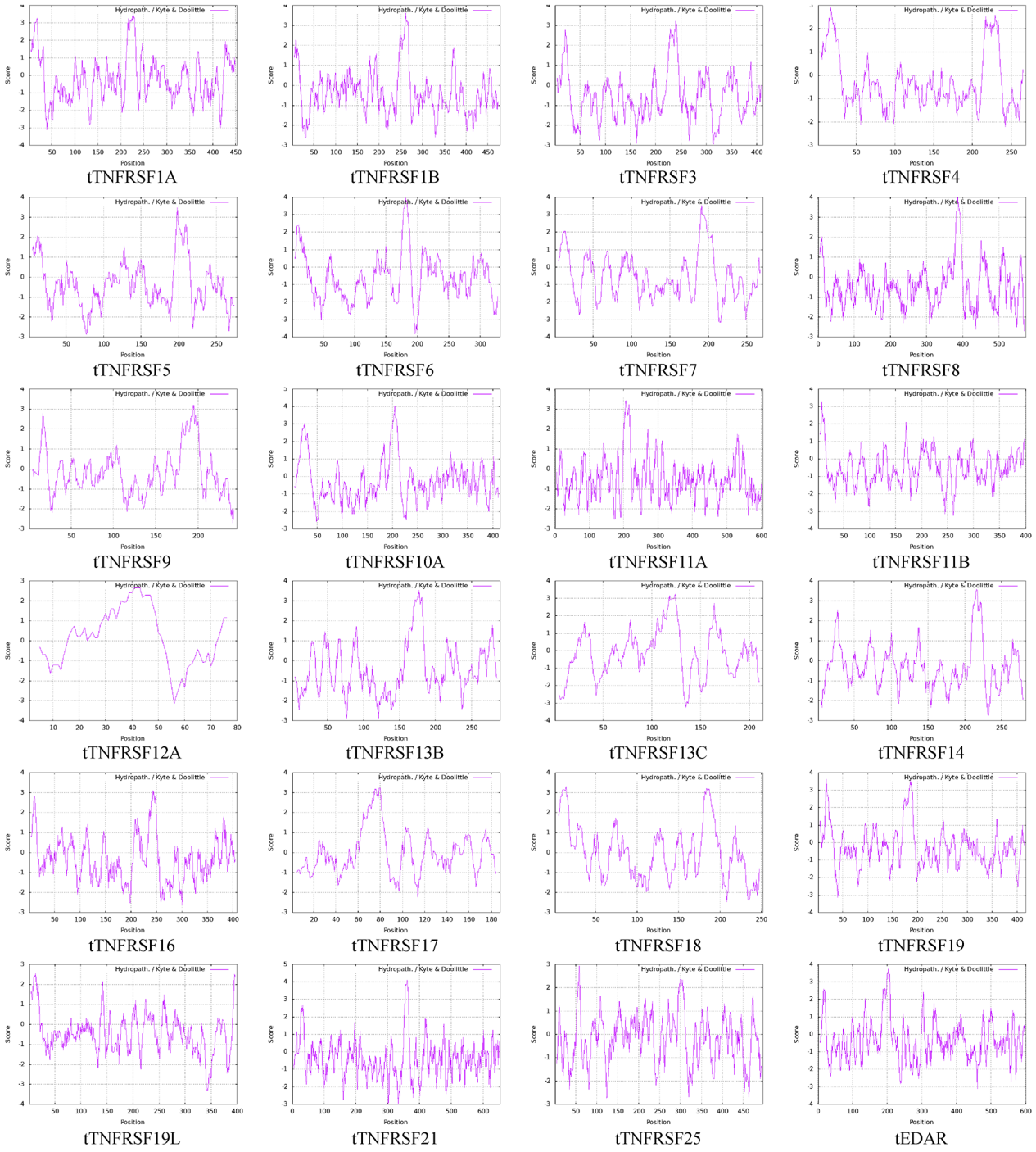

Fig. 3 Hydropathy index distribution chart of the 24 TNFRSF receptors in tree shrews. The x-axis represents the amino acid position, while the y-axis represents the hydropathy index. Positive scores indicate hydrophobicity, while negative scores indicate hydrophilicity. The higher the absolute value, the greater the degree of hydrophobicity/hydrophilicity

shrews. After data quality control and alignment with the tree shrew reference genome, the gene expression profile for each sample was obtained. Figure 5A shows a heatmap of TNFRSF gene expressions across various tree shrew organs. TNFRSF genes were ubiquitously expressed in all six tissues, with individual members presenting tissue-specific expression patterns. Notably, higher expression levels were observed in immune

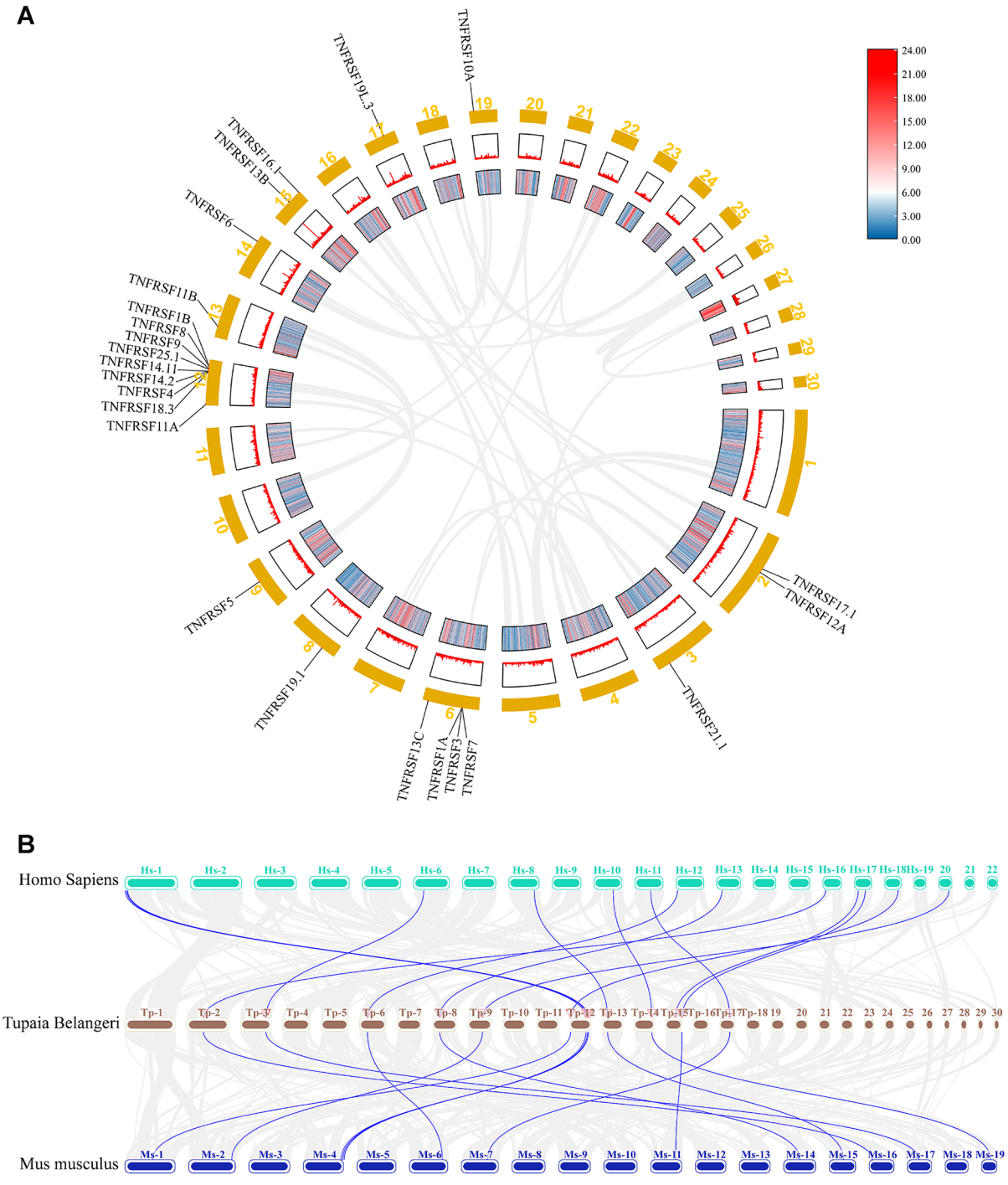

Fig. 4 Chromosomal localization and collinearity analysis of the TNFRSF genes. (**A**) Chromosomal localization of TNFRSF genes in tree shrews. The outer circle in yellow represents chromosomes, the middle circle indicates the gene density histogram of chromosomes, the inner circle shows the gene density of chromosomes, and the central gray arc represents all collinear genes in tree shrews. (**B**) Genomic collinearity analysis map of tree shrew, human, and mouse. Green, brown, and blue squares represent the chromosomes of humans, tree shrews, and mice, respectively. Gray lines indicate regions of collinearity between humans, tree shrews, and mice. Blue lines represent collinear gene pairs among TNFRSF genes

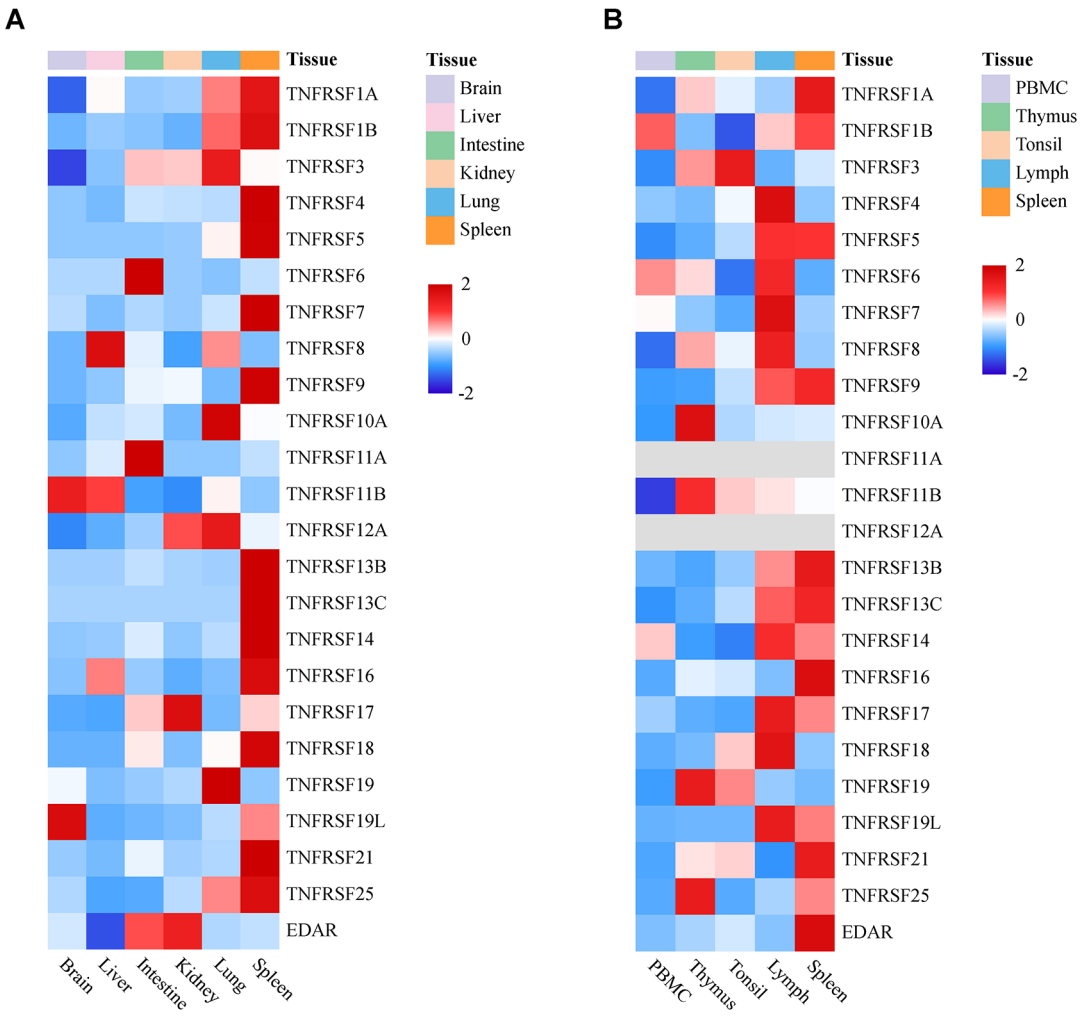

Fig. 5 Expression profiles of tTNFRSF genes in various tissues. (**A**) Transcriptional data from the brain, liver, small intestine, kidney, lung, and spleen of tree shrews were retrieved through literature searches. A heatmap of TNFRSF gene expression profiles was generated based on the selected data. (**B**) Transcriptional data from peripheral blood mononuclear cells (PBMCs), thymus, tonsils, lymph nodes, and spleen of tree shrews were analyzed to create a heatmap of TNFRSF gene expression profiles in these five immune cells or tissues, where gray squares represent expression values of 0

organs. TNFRSF17 was significantly expressed in the kidney tissue, whereas TNFRSF11B and TNFRSF8 were prevalent in the liver tissue. Meanwhile, TNFRSF11B and TNFRSF19L were highly expressed in the brain tissues. In contrast, both TNFRSF1A and TNFRSF3 exhibited lower expressions in the brain tissue, and EDAR expression was reduced in the liver tissue.

Regarding expression in immune organs (Fig. 5B), TNFRSF1A, TNFRSF3, TNFRSF5, TNFRSF9, TNFRSF13B, TNFRSF13C, TNFRSF16, TNFRSF21, and EDAR exhibited the highest expression in the spleen. TNFRSF4, TNFRSF6, TNFRSF7, TNFRSF8, TNFRSF14, TNFRSF17, TNFRSF18, and TNFRSF19L showed the highest expression in lymph nodes. TNFRSF3 showed the highest expression in the tonsils, whereas TNFRSF10A, TNFRSF11B, TNFRSF19, and TNFRSF25 displayed the highest expression in the thymus. TNFRSF11B exhibited the lowest expression levels in PBMC. TNFRSF11A and TNFRSF12A were not detected in the immune organs, which is consistent with the results reported by Ye et al.[4] Furthermore, a protein-protein interaction (PPI) network of 24 members of tTNFRSF was constructed using the STRING database. The DMNC and Stress algorithms from the Cytoscape plugin cytoHubba were used to score genes and identify the hub genes. The intersection of the top ten genes identified by both algorithms, including TNFRSF4, TNFRSF7, TNFRSF13C, and TNFRSF25, was chosen as the key gene. To determine the relative expression levels of these genes, we performed RT-qPCR analysis on eight tree shrew tissues. RT-qPCR was conducted to evaluate the relative expression levels of TNFRSF4, TNFRSF7, TNFRSF13C, and TNFRSF25 in

those tissues (Fig. 6). The results showed that these genes were most highly expressed in the spleen tissue, consistent with our RNA-seq results. Additionally, immunofluorescence experiments were conducted to visualize the co-expression of TNFRSF13C with the B cell surface marker CD79A in the spleen, lymph nodes, and tonsils. As shown in Fig. 7, TNFRSF13C and CD79A co-localized in all three targeted tissues of the tree shrew, consistent with the existing literature.

Expression pattern of tTNFRSF genes in tree shrew after viral infection

TNFRSF plays important roles in host immune defense, inflammatory responses, and signal transduction pathways and is involved in antiviral processes during viral infections. To study the effects of TNFRSF on viral infection, healthy adult tree shrews were intravenously inoculated with an EBV suspension or an equal volume of virus-free RPMI 1640 medium. They were euthanized at different time points: before infection, on day 7 post-infection, and on day 28 post-infection ($n = 3$). Peripheral blood was collected, and mononuclear cells were isolated to extract RNA for transcriptome sequencing. The

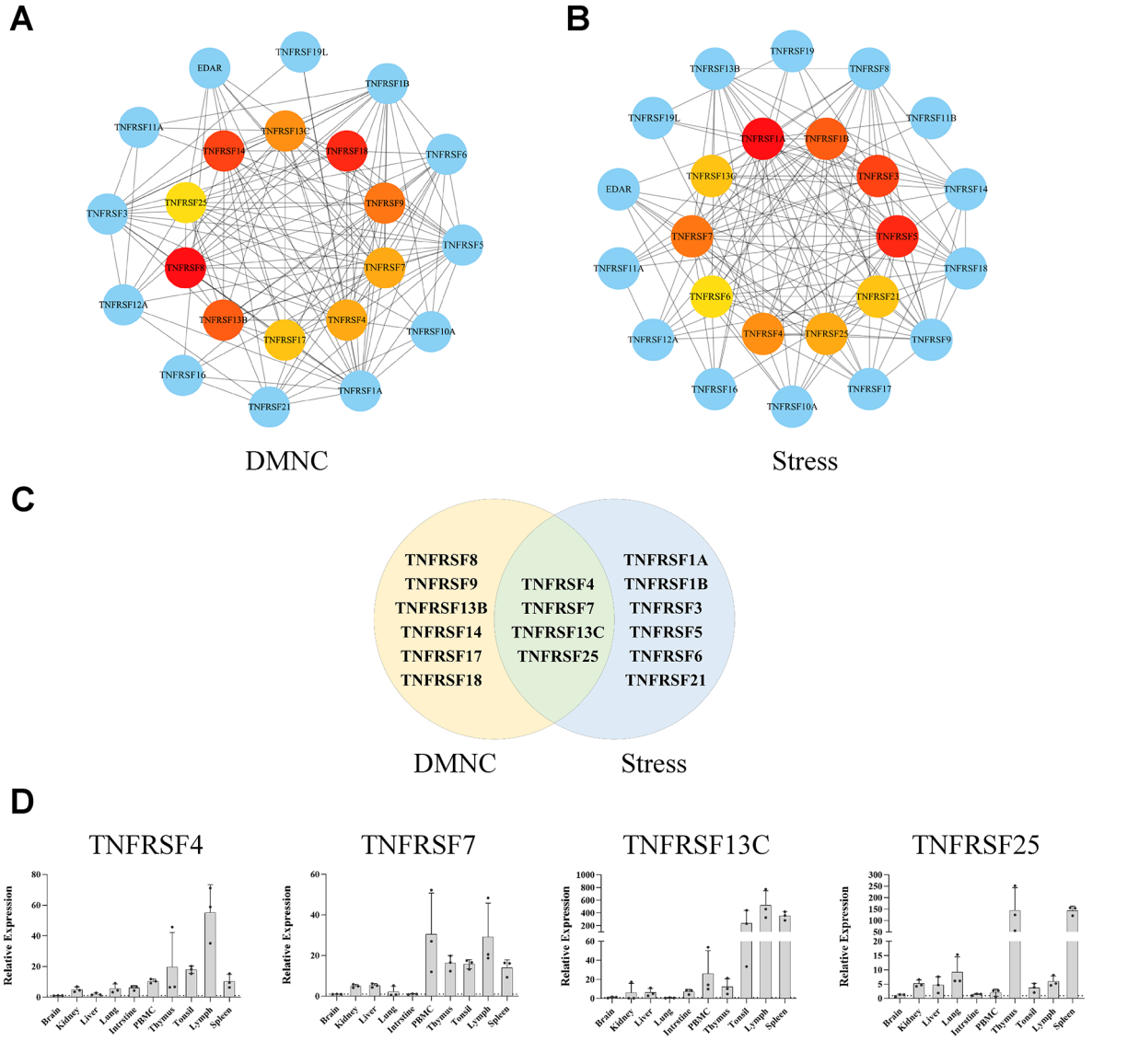

Fig. 6 Visualizing the PPI network of the tree shrew TNFRSF genes using Cytoscape. The cytoHubba plugin was utilized to filter hub genes based on DMNC (**A**) and Stress (**B**) scores. In the network, blue nodes represent genes, connecting lines indicate interactions between genes, and hub genes are represented by red and yellow nodes, with the score magnitude transitioning from red to yellow. Genes with overlapping DMNC and Stress scores were identified as the key genes (**C**). Subsequently, RT-qPCR was conducted to validate the relative mRNA expression of these key genes, TNFRSF4, TNFRSF7, TNFRSF13C, and TNFRSF25, in different tissues (**D**)

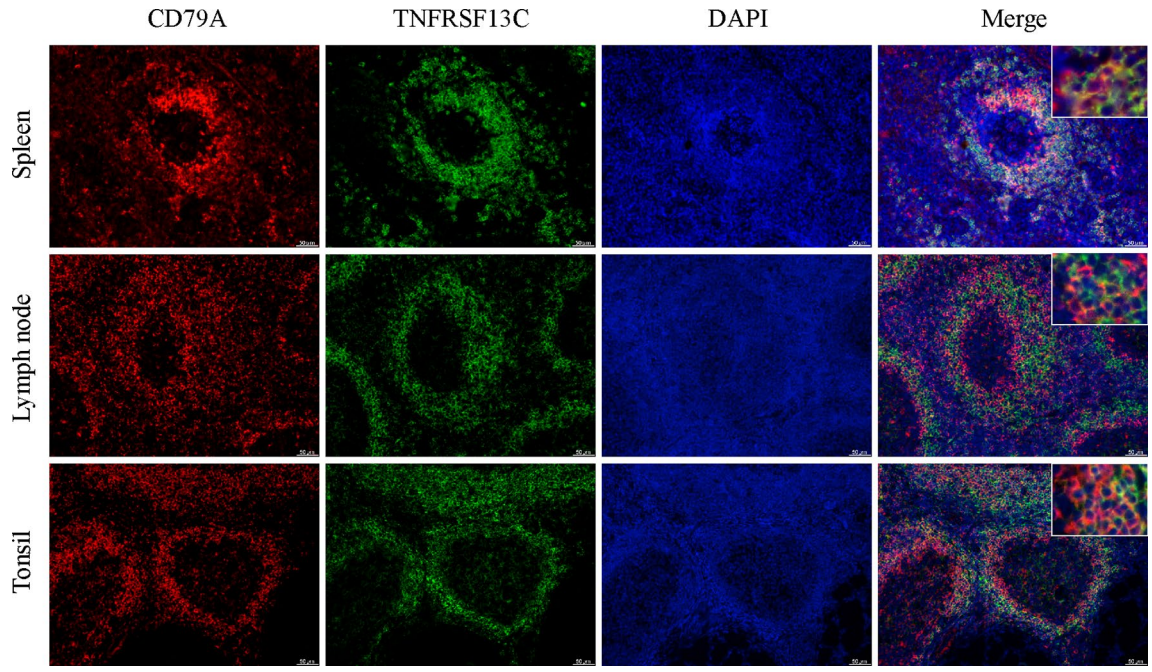

Fig. 7 Using immunofluorescence experiments, the co-expression of TNFRSF13C and CD79A was observed in paraffin sections of tree shrew spleen, lymph nodes, and tonsils. CD79A, a B cell surface receptor expressed on the cell membrane, appears as red fluorescence in the images. TNFRSF13C, expressed on the cell membrane, appears as green fluorescence. The cell nuclei were stained with DAPI, appearing as blue fluorescence. After merging the fluorescence channels, areas of co-expression of CD79A and TNFRSF13C are shown as orange fluorescence

raw sequencing data were quality controlled and aligned to the reference genome to obtain the gene expression profiles of tree shrews at different time points after EBV infection. Additionally, literature searches were conducted to collect information on the responses and mRNA changes in different tissues or organs of tree shrews to various viral infections, including hepatitis B, hepatitis C, coxsackievirus, Newcastle disease virus, and Sendai virus. The details are presented in Table S8.

The expression levels of the 24 members of TNFRSF in tree shrew tissues or cells infected with different viruses were standardized. As shown in Figs. 8A and 28 days after EBV inoculation, TNFRSF5 and TNFRSF14 were significantly upregulated ($p < 0.05$), whereas TNFRSF19 was significantly downregulated. When tree shrew hepatocytes were co-cultured with HCV for 24 h in vitro, TNFRSF9 was significantly upregulated and TNFRSF21 was significantly downregulated. After 48 h of infection, the expression of TNFRSF1A, TNFRSF1B, TNFRSF7, and TNFRSF9 was significantly upregulated. Following co-culture with TSPRC and EMCV for 3 h, TNFRSF13C and TNFRSF1A were significantly upregulated after 12 h. Co-culture of TSPRC and NDV for 12 h resulted in significant upregulation of TNFRSF7 and TNFRSF10A. Meanwhile, TNFRSF1A, TNFRSF1B, TNFRSF11B, and TNFRSF21 were significantly upregulated after co-culture with TSPRC and SeV for 3 h. TNFRSF13C was significantly upregulated after 9 h of co-culture, whereas TNFRSF10A and TNFRSF11B were significantly downregulated. After 12 h, TNFRSF1B and TNFRSF10 expression was significantly upregulated. To investigate the common and specific changes in TNFRSF genes after viral infection, the upregulated TNFRSF genes were extracted. An upset plot (Fig. 8B) shows that eight genes were upregulated after different viral infections, including TNFRSF1A, TNFRSF1B, TNFRSF3, TNFRSF5, TNFRSF7, TNFRSF13B, TNFRSF14, and TNFRSF19L, suggesting that these genes may act synergistically during viral infections.

Function of the tTNFRSF genes in tree shrews during EBV infection

To gain further insight into the regulatory pathways and mechanisms involving TNFRSF genes during viral infections in tree shrews, relevant literature was reviewed to summarize potential downstream pathways that TNFRSF genes may activate, including the NF-κB, MAPK, JNK, mTOR, and apoptosis signaling pathways [33, 44, 45]. Gene set enrichment analysis (GSEA) was conducted on the gene expression profiles of tree shrews infected with EBV using single-sample gene set enrichment analysis (ssGSEA). The gene sets were derived from classification databases provided by the official GSEA website, such as the Hallmark gene set, C2 curated gene set-KEGG, and C5 GO gene set-BP, as well as from our custom dataset comprising 24 TNFRSF genes of tree shrews.

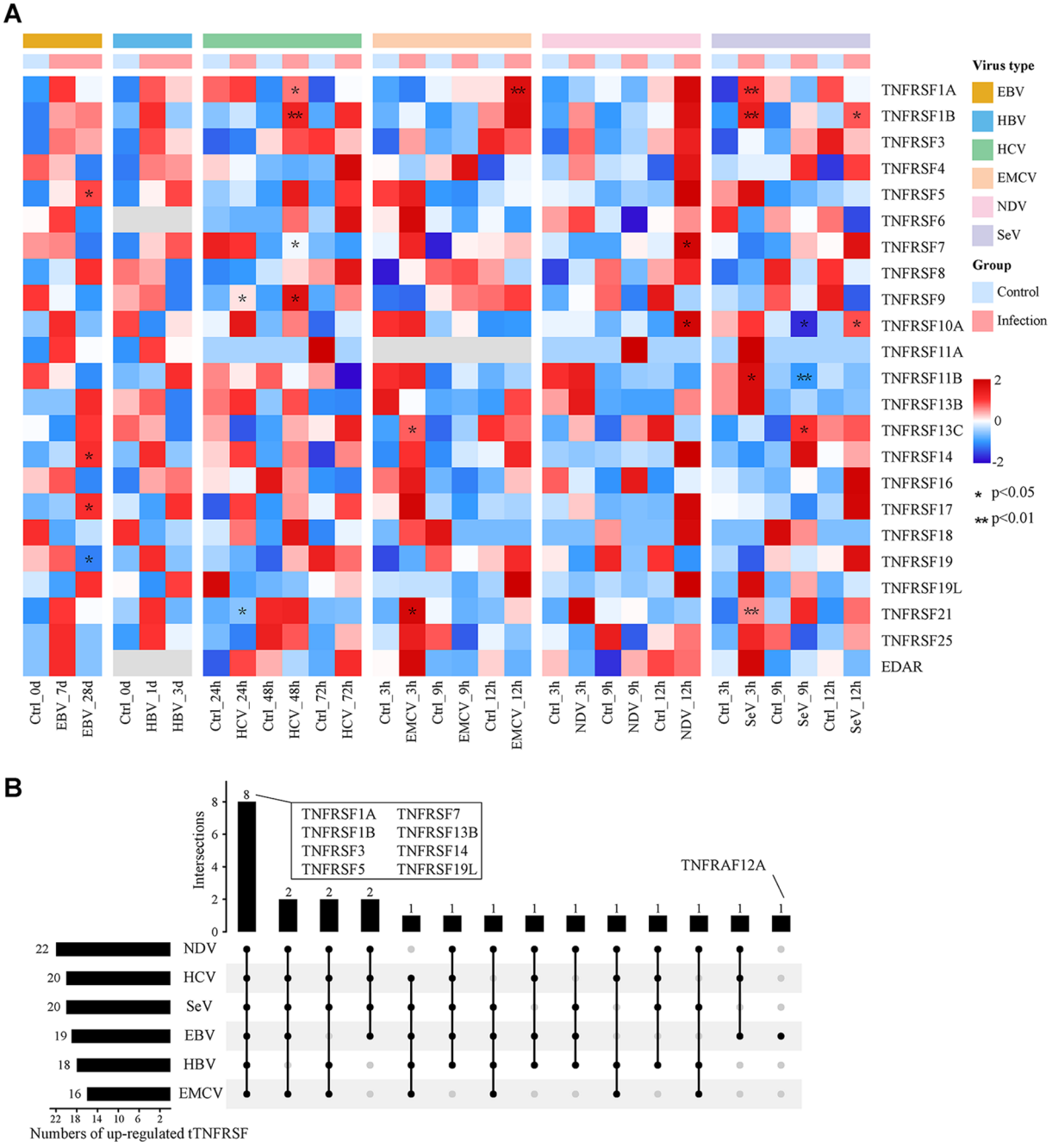

Fig. 8 Changes in the expression of TNFRSF genes in tree shrews following viral infection. (**A**) Analysis of transcriptome data from an established EBV infection model by our research group, along with a literature retrieval of transcriptome data from five viral infection models, was conducted to determine the changes in TNFRSF mRNA expressions before and after infection. Genes with significantly different expression are indicated with an asterisk*, where *$p < 0.05$ and **$p < 0.01$. (**B**) An UpSet plot displays the number of upregulated TNFRSF genes after different viral infections. The horizontal bar graph illustrates the total count of upregulated TNFRSF genes after different viral infections. Black dots and lines represent upregulated genes specific to or shared among different viral infections. The numbers on the vertical bar graph indicate the count of specific or shared upregulated genes. NDV, Newcastle disease virus; HCV, hepatitis C virus; SeV, Sendai virus; EBV, Epstein-Barr virus; HBV, hepatitis B virus; EMCV, encephalomyocarditis virus

Subsequently, ssGSEA scores related to the above-mentioned signaling pathways were selected from these datasets, revealing significant enrichment of these pathways in the transcriptome data after EBV infection, albeit with varying degrees of enrichment.

We subsequently conducted a correlation analysis between the expression levels of our selected key core hub genes and the ssGSEA scores. The results indicate significant correlations between TNFRSF1A, TNFRSF3, and TNFRSF19L with the NF-κB pathway (Fig. 9). Their

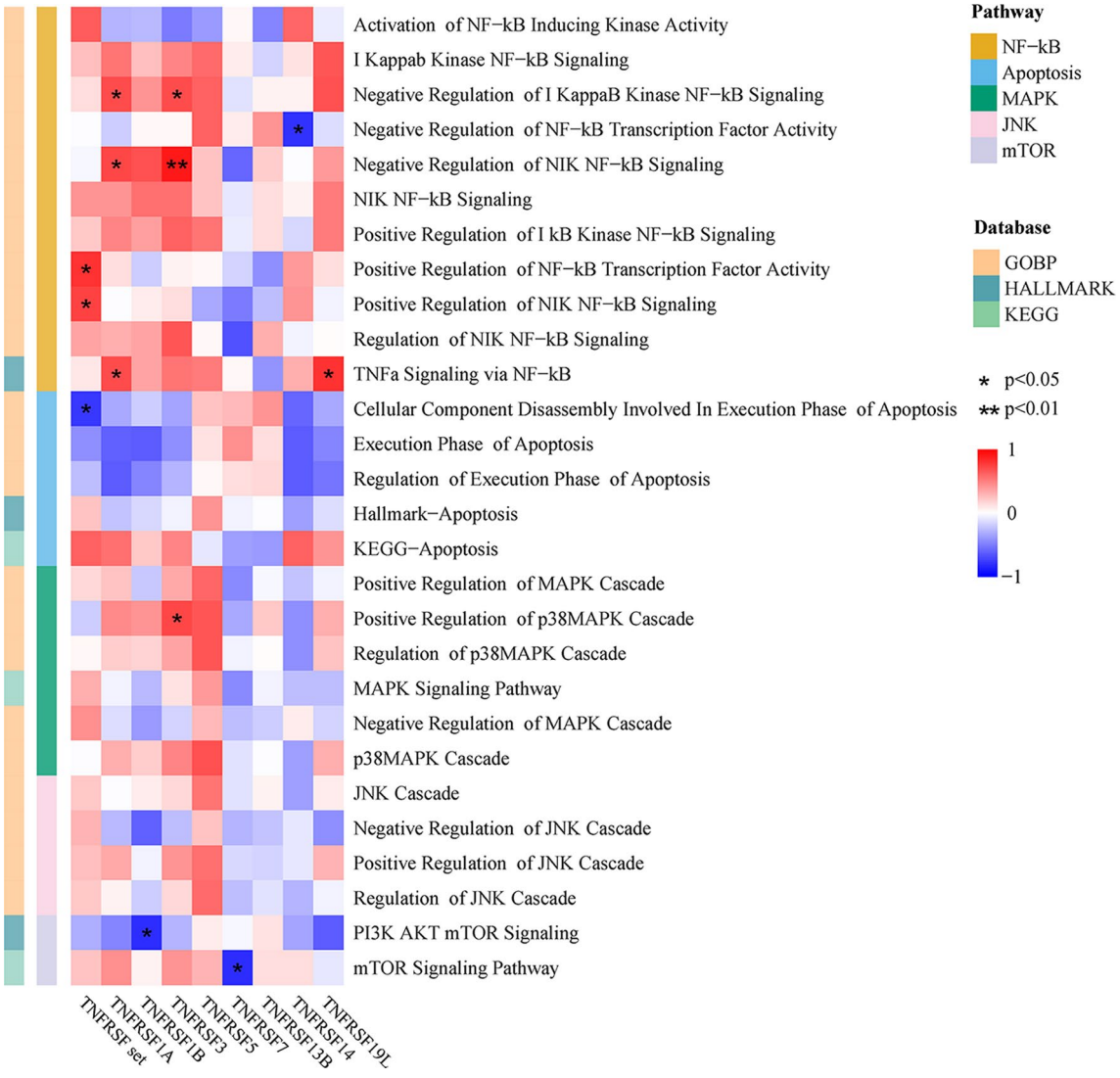

Fig. 9 Functional analysis of the TNFRSF members in tree shrews following EBV infection. Single-sample gene set enrichment analysis (ssGSEA) was performed on PBMC transcriptome data before and after EBV infection in tree shrews. The ssGSEA scores, which were related to TNFRSF gene function (NF-κB, MAPK, JNK, mTOR, and apoptosis signaling pathways), were correlated with the expression levels of TNFRSF genes in the corresponding samples. In the heatmap, the degree of correlation is represented by red and blue colors, indicating high and low correlation, respectively. Significance of correlation is denoted by asterisks, where $*p < 0.05$ and $**p < 0.01$

expression levels were positively associated with the "Negative Regulation of IKK NF-κB Signaling" in the GO-BP biological process dataset and the "TNFα Signaling via NF-κB" pathway in the Hallmark dataset. Additionally, TNFRSF14 exhibited a significant negative correlation with the "Negative Regulation of NF-κB Transcription Factor Activity" pathway in the GO-BP dataset. Furthermore, by considering all tTNFRSF genes as a custom gene set, a correlation analysis between the ssGSEA scores of the TNFRSF gene set and the scores of the aforementioned pathways revealed a positive association with "Positive Regulation of NF-kB Transcription Factor Activity" and "Positive Regulation of NIK NF-kB Signaling," while displaying a negative correlation with the apoptosis pathway ($p < 0.05$).

Discussion

Owing to their unique phylogenetic proximity to primates, tree shrews are increasingly gaining recognition as valuable alternative animal models in biomedical research. Despite improvements in understanding the tree shrew genome, which has expedited the development of human disease models using these animals [4, 46], our knowledge of tree shrew evolution and genetics remains limited. For instance, research on the tree shrew immune system through whole-genome sequencing has revealed the loss of the innate immune receptor gene RIG-I, which

is known to activate the MAVS signaling pathway, as well as the NF-κB pathway to produce interferons [3]. Consequently, the immune response is interrupted, potentially rendering tree shrews more susceptible to pathogenic infections. Further, Xu et al. discovered the interaction between tMDA5 and the adaptor tMITA (binds exclusively with RIG-I), which partially compensates for the loss of RIG-I and its function, providing insights into the adaptability and functional diversity of the tree shrew innate immune response [47]. Additionally, an increasing number of immune-related genes or gene families have been identified and characterized in tree shrews, such as GBP, IL6, IL7, TLR, and the OSA gene family [48–51], deepening our understanding of the immune response in this animal and enhancing its value as a study model. In the present study, we identified 24 tree-shrew TNFRSF genes. As expected, the tTNFRSF genes aligned more closely with human TNFRSF genes in the phylogenetic tree. Thus, these tTNFRSF genes have not undergone positive selection, suggesting their relative conservation. Furthermore, TNFRSF genes in tree shrews exhibit some unique characteristics.

Research on the TNFRSF superfamily of cytokine receptors can be traced back to studies in Drosophila melanogaster, where orthologs of this gene family have been identified. These studies provide valuable insights into the evolutionary conservation and functional diversity of TNFRSF across species [52]. Studies on the fruit fly genome have identified the TNFRSF ortholog, Wengen, and its ligand, Eiger [53]. In the process of biological evolution, single biological behaviors, such as cell apoptosis pathway, may prove insufficient to satisfy the evolutionary needs of a species. Gene duplication, as the main driver of gene family expansion, facilitates the creation of novel apoptotic pathways and functions, enabling cells to adapt for survival and evolution. While other mechanisms, such as genome duplication, also contribute to gene family expansion, gene duplication remains the predominant method underlying this process. Most members within a gene family have similar structures and/or functions. In the present study, the positions of motif1, 2, and 3 highly overlapped with the TNFR domain region, suggesting that these motifs are alternative expressions of the TNFR domain. Motif1, 2, and 3 are cysteine-rich conserved motifs. The cysteine-rich region in motif1, 2, and 3 is likely the CRD, which is the TNFR-binding domain. Notably, Motif7, which is prevalent in TNFRSF1A, 9, 13B, 13 C, 17, 25, and EDAR, is also rich in cysteine, suggesting that it may also serve as a TNFR-binding domain. A conserved motif from the DD superfamily was observed in tTNFRSF1A, 6, 10 A, 16, 21, 25, and EDAR. A Death superfamily was identified in tTNFRSF11B. Interestingly, the same eight genes also possess a DD in humans. TNFRSF13C, also referred to as the B cell activation factor receptor (BAFFR), exhibits a Motif7 structure in the tree shrew version that overlaps considerably with the BAFFR-TALL-BIND superfamily site region. This overlap suggests that the Motif7 region of the tTNFRSF13C could constitute the active region of BAFFR, thereby facilitating B cell maturation via binding with BAFF within this area.

Most TNFRSF genes showed high expression levels within the immune system tissues of tree shrews, which is consistent with related studies on their distribution in human tissues. Such expression prevalence in the immune tissues of tree shrews suggests potential advantages for devising human disease models, thereby displaying the critical roles that TNFRSF members play in immune regulation, signal transduction, and defense mechanisms against pathogen intrusions. The varying distribution of TNFRSF genes in different tissues reflects their diverse roles in physiological and pathological processes, which are crucial for understanding their biological functions. Remarkably, TNFRSF19 is highly expressed in the airway epithelium and brain tissues but less expressed in major lymphoid tissues such as the spleen. Its widespread application in the nervous system, along with its uniquely high abundance in neural stem cells and astrocytes, suggests that TNFRSF19 may exclude its direct involvement in immune regulation [54]. For instance, TNFRSF19 can act as an alternative to p75 in the NgR1/p75/LINGO-1 complex, replacing p75 with NgR1 and activating the RhoA signaling pathway in Cos7 cells, thereby transducing neuronal inhibitory signals [55]. In our study, we found that despite TNFRSF19 lacking an intracellular DD and being a non-death receptor in tree shrews, its intracellular region encompassed TNFRSF-binding sequences capable of activating the NF-κB signaling pathway, ultimately inducing apoptosis.

After viral infection, the pattern recognition receptors in host cells identify pathogenic components such as viral RNA or DNA. Activated pattern recognition receptors recruit and activate a series of signaling molecules or cytokines through their intracellular domains. Upon binding of the TNF ligand to the TNF receptor on the cell surface, the silencer of death domain (SODD) protein dissociates from the DD of the TNF receptor, exposing the DD that recruits the TNFR-related death domain (TRADD) protein and induces the formation of the TNFR-TRADD-RIP1-TRAF2 complex [56]. This complex can activate the NF-κB signaling pathway, promote the transcription of target genes, resist apoptosis, and promote cell survival. In addition, TNF ligands can be internalized via clathrin. Internalized TNF binds to TRADD and FAS-associated death domain protein (FADD) in the cytoplasm, forming the DISC signal complex, activating caspase-8 and leading to apoptosis or programmed necrosis of infected cells [34]. We found that tree shrews

could combat viral invasion by regulating various signaling pathways after EBV infection. The NF-κB signaling pathway is the primary downstream pathway, similar to that in humans. Interestingly, the expression of TNFRSF14 decreased post-EBV infection and held a significant negative correlation with the Negative Regulation of NF-κB Transcription Factor Activity. This may be due to the bidirectional biological characteristics of the TNFRSF, as mentioned previously. TNFRSF14, also known as a herpes virus entry mediator (HVEM), serves as an immunoregulatory molecule and is a specific receptor for B and T lymphocyte attenuators, exhibiting bidirectional regulatory characteristics that promote and inhibit inflammatory reactions [57]. This remains vital for the host's antiviral response but also provides a potential opportunity for viruses to deflect immune surveillance or assist viral replication.

We found that TNFRSF12A is specifically upregulated during EBV infection, which may be related to the unique mechanism of EBV infection. This distinct expression pattern may also indicate special alterations in cellular signaling pathways during EBV infection, which significantly contribute to the pathogenesis of EBV-associated conditions, thereby necessitating further investigation. In cancer research, TNFRSF agonists are being explored as immunotherapeutic agents intended to amplify the immune system's attack on tumor cells by activating TNFRSF members. Currently, various TNFRSF agonists are undergoing clinical trials to determine their safety, efficacy, and optimal dosage. These agonists can simulate natural ligands by promoting the proliferation, survival, and cytotoxicity of immune cells, such as T and natural killer (NK) cells, to enhance the antitumor immune response. Considering the potential of TNFRSF agonists in regulating immune responses, their application in the treatment of viral infectious diseases was also explored in the present study.

Although tTNFRSF shares structural and functional similarities with human TNFRSF, unique ligand recognition patterns may be present in TNFRSF; thus, hTNFRSF agonists may not necessarily activate tTNFRSF. Based on their tissue dispersion patterns, TNFRSFs are primarily expressed in tree shrew immune cells. However, isolating and immortalizing tree shrew immune cells are challenging. Therefore, we did not conduct predictions or comparisons of tree shrew TNFRSF ligands in this study. Further research on how various TNFRSF agonists activate the NF-κB signaling pathway in tree shrew immune cells would be valuable.

The identification of TNFRSF presents significant challenges due to the inherent differences between gene superfamilies and gene families. Specifically, the low sequence similarity among TNFRSF members limits the efficacy of sequence-based identification approaches. Moreover, the functional diversification and evolutionary differentiation of TNFRSF members increase the risk of misclassification or omission of certain genes, potentially compromising the comprehensiveness and accuracy of studies. These challenges are further exacerbated in non-model organisms, particularly those with incomplete genome annotations. Fortunately, the annotation of tree shrew genome used for this study is more comprehensive than previous versions, significantly enhancing the reliability and completeness of the results of this study.

Conclusion

We conducted a comprehensive analysis of the tree shrew genome, including 24 tTNFRSF genes, revealing their structure, conserved motifs, physicochemical properties, evolutionary relationships, and tissue expression patterns, which may be relevant to biological functions. These results suggest a closer phylogenetic relationship between tTNFRSF genes and those of humans. Within the tree shrew viral infection model, TNFRSF genes exert antiviral functions most likely via the activation of the NF-κB pathway. Our study has the potential to advance the understanding of the roles of TNFRSF genes in tree shrew-human viral infection models and provide valuable insights into the development of antiviral drugs or vaccines.

Supplementary Information

The online version contains supplementary material available at https://doi.org/10.1186/s12864-025-11451-x.

Supplementary Material 1
Supplementary Material 2
Supplementary Material 3
Supplementary Material 4
Supplementary Material 5
Supplementary Material 6
Supplementary Material 7
Supplementary Material 8

Acknowledgements

We thank the Experimental Animal Center of Guangxi Medical University for providing technical support for animal feeding. We thank the members of our research groups for providing technical Assistance and participating in discussions.

Author contributions

Z. H and N. S performed data and laboratory analyses. Z. L and F. C provided tissue samples and performed experiments. X. F, J. L and Y. L performed cell culture. N. S, W. X and Z. H drafted the manuscript and participated in the preparation of its final version. W. X designed and supervised the whole project. A. T supervised the work. A. T, X. Y, N. S and Z, L were responsible for funding acquisition. All authors reviewed the manuscript.

Funding

This study was supported by the National Natural Science Foundation of China (No. 32060132 and 82260519), National Natural Science United

Foundation of China (No. U21A20371), Guangxi Clinic Medicine Research Center of Nasopharyngeal Carcinoma (grant GuikeAD20297078), Innovation Project of Guangxi Graduate Education (No. YCBZ2024120 and No. YCSW2024267) and Guangxi Key Laboratory of Early Prevention and Treatment for Regional High Frequency Tumor (Guangxi Medical University) (No. GKE-ZZ202225 and No.GKE-ZZ202301).

Data availability

The datasets used in this study are available in the following online repositories with accession number PRJNA1127584 for https://www.ncbi.nlm.nih.gov/.

Declarations

Ethics approval and consent to participate

All animal experiments were performed in strict accordance with the ARRIVE guidelines and Basel Declaration ethical standards, with particular emphasis on the "3R" principle (Replacement, Reduction, and Refinement). The study protocols were reviewed and approved by the Institutional Review Board of the Guangxi Medical University (No. 202201010).

Consent for publication

Not applicable.

Competing interests

The authors declare no competing interests.

Received: 29 October 2024 / Accepted: 5 March 2025
Published online: 04 April 2025

References

1. Xiao J, Liu R, Chen CS. Tree shrew (Tupaia belangeri) as a novel laboratory disease animal model. Zoological Res. 2017;38(3):127–37.
2. Yao YG. Creating animal models, why not use the Chinese tree shrew (Tupaia belangeri chinensis)? Zoological Res. 2017;38(3):118–26.
3. Fan Y, Huang ZY, Cao CC, Chen CS, Chen YX, Fan DD, He J, Hou HL, Hu L, Hu XT, et al. Genome of the Chinese tree shrew. Nat Commun. 2013;4:1426.
4. Ye MS, Zhang JY, Yu DD, Xu M, Xu L, Lv LB, Zhu QY, Fan Y, Yao YG. Comprehensive annotation of the Chinese tree shrew genome by large-scale RNA sequencing and long-read isoform sequencing. Zoological Res. 2021;42(6):692–709.
5. Li R, Xu W, Wang Z, Liang B, Wu JR, Zeng R. Proteomic characteristics of the liver and skeletal muscle in the Chinese tree shrew (Tupaia belangeri chinensis). Protein Cell. 2012;3(9):691–700.
6. Xu L, Chen SY, Nie WH, Jiang XL, Yao YG. Evaluating the phylogenetic position of Chinese tree shrew (Tupaia belangeri chinensis) based on complete mitochondrial genome: implication for using tree shrew as an alternative experimental animal to primates in biomedical research. J Genet genomics = Yi Chuan Xue Bao. 2012;39(3):131–7.
7. Xia W, Huang ZJ, Shi N, Feng YW, Tang AZ. Dosage selection and effect evaluation of sodium pentobarbital in tree shrew anesthesia. Lab Anim. 2023;57(3):283–92.
8. Shi N, Xia W, Ji K, Feng Y, Li H, He G, Tang A. Anatomy and nomenclature of tree shrew lymphoid tissues. Exp Anim. 2022;71(2):173–83.
9. Xia W, Huang ZJ, Feng YW, Tang AZ, Liu L. Body surface area-based equivalent dose calculation in tree shrew. Sci Prog. 2021;104(2):368504211016935.
10. Ni RJ, Huang ZH, Luo PH, Ma XH, Li T, Zhou JN. The tree shrew cerebellum atlas: systematic nomenclature, neurochemical characterization, and afferent projections. J Comp Neurol. 2018;526(17):2744–75.
11. Zhang J, Luo RC, Man XY, Lv LB, Yao YG, Zheng M. The anatomy of the skin of the Chinese tree shrew is very similar to that of human skin. Zoological Res. 2020;41(2):208–12.
12. Feng Y, Xia W, Ji K, Lai Y, Feng Q, Chen H, Huang Z, Yi X, Tang A. Hemogram study of an artificially feeding tree shrew (Tupaia belangeri chinensis). Exp Anim. 2020;69(1):80–91.
13. Xia W, Huang ZJ, Guo ZL, Feng YW, Zhang CY, He GY, Tang AZ. Plasma volume, cell volume, total blood volume and F factor in the tree shrew. PLoS ONE. 2020;15(9):e0234835.
14. Chen G, Wang W, Meng S, Zhang L, Wang W, Jiang Z, Yu M, Cui Q, Li M. CXC chemokine CXCL12 and its receptor CXCR4 in tree shrews (Tupaia belangeri): structure, expression and function. PLoS ONE. 2014;9(5):e98231.
15. Zhang J, Xiao H, Bi Y, Long Q, Gong Y, Dai J, Sun M, Cun W. Characteristics of the tree shrew humoral immune system. Mol Immunol. 2020;127:175–85.
16. Xia W, Chen H, Feng Y, Shi N, Huang Z, Feng Q, Jiang X, He G, Xie M, Lai Y, et al. Tree shrew is a suitable animal model for the study of epstein barr virus. Front Immunol. 2021;12:789604.
17. Yuan B, Yang C, Xia X, Zanin M, Wong SS, Yang F, Chang J, Mai Z, Zhao J, Zhang Y, et al. The tree shrew is a promising model for the study of influenza B virus infection. Virol J. 2019;16(1):77.
18. Shi N, Chen H, Lai Y, Luo Z, Huang Z, He G, Yi X, Xia W, Tang A. Cyclosporine A induces Epstein-Barr virus reactivation in tree shrew (Tupaia belangeri chinensis) model. Microbes Infect. 2023;25(8):105212.
19. Wang E, Ye Y, Zhang K, Yang J, Gong D, Zhang J, Hong R, Zhang H, Li L, Chen G, et al. Longitudinal transcriptomic characterization of viral genes in HSV-1 infected tree shrew trigeminal ganglia. Virol J. 2020;17(1):95.
20. Li R, Yuan B, Xia X, Zhang S, Du Q, Yang C, Li N, Zhao J, Zhang Y, Zhang R, et al. Tree shrew as a new animal model to study the pathogenesis of avian influenza (H9N2) virus infection. Emerg Microbes Infections. 2018;7(1):166.
21. Wang Z, Yi X, Du L, Wang H, Tang J, Wang M, Qi C, Li H, Lai Y, Xia W, Tang A. A study of Epstein-Barr virus infection in the Chinese tree shrew(Tupaia belangeri chinensis). Virol J. 2017;14(1):193.
22. Jiang L, Lu C, Sun Q. Tree shrew as a new animal model for the study of dengue virus. Front Immunol. 2021;12:621164.
23. Zhang L, Shen ZL, Feng Y, Li DQ, Zhang NN, Deng YQ, Qi XP, Sun XM, Dai JJ, Yang CG, et al. Infectivity of Zika virus on primary cells support tree shrew as animal model. Emerg Microbes Infections. 2019;8(1):232–41.
24. Yang C, Ruan P, Ou C, Su J, Cao J, Luo C, Tang Y, Wang Q, Qin H, Sun W, Li Y. Chronic hepatitis B virus infection and occurrence of hepatocellular carcinoma in tree shrews (Tupaia belangeri chinensis). Virol J. 2015;12:26.
25. Feng Y, Feng YM, Lu C, Han Y, Liu L, Sun X, et al. Tree shrew, a potential animal model for hepatitis C, supports the infection and replication of HCV in vitro and in vivo. J Gen Virol. 2017;98(8):2069–78.
26. Yi J, Lei X, Guo F, Chen Q, Chen X, Zhao K, Zhu C, Cheng X, Lin J, Yin H, Xia Y. Co-delivery of Cas9 mRNA and guide RNAs edits hepatitis B virus episomal and integration DNA in mouse and tree shrew models. Antiviral Res. 2023;215:105618.
27. Li CH, Yan LZ, Ban WZ, Tu Q, Wu Y, Wang L, Bi R, Ji S, Ma YH, Nie WH, et al. Long-term propagation of tree shrew spermatogonial stem cells in culture and successful generation of Transgenic offspring. Cell Res. 2017;27(2):241–52.
28. Hehlgans T, Pfeffer K. The intriguing biology of the tumour necrosis factor/tumour necrosis factor receptor superfamily: players, rules and the games. Immunology. 2005;115(1):1–20.
29. Wajant H, Pfizenmaier K, Scheurich P. Tumor necrosis factor signaling. Cell Death Differ. 2003;10(1):45–65.
30. Idriss HT, Naismith JH. TNF alpha and the TNF receptor superfamily: structure-function relationship(s). Microsc Res Tech. 2000;50(3):184–95.
31. Sukits SF, Lin LL, Hsu S, Malakian K, Powers R, Xu GY. Solution structure of the tumor necrosis factor receptor-1 death domain. J Mol Biol. 2001;310(4):895–906.
32. Park YH, Jeong MS, Jang SB. Structural insights of homotypic interaction domains in the ligand-receptor signal transduction of tumor necrosis factor (TNF). BMB Rep. 2016;49(3):159–66.
33. Yang CM, Yang CC, Hsu WH, Hsiao LD, Tseng HC, Shih YF. Tumor necrosis Factor-α-Induced C-C motif chemokine ligand 20 expression through TNF receptor 1-Dependent activation of EGFR/p38 MAPK and JNK1/2/FoxO1 or the NF-κB pathway in human cardiac fibroblasts. Int J Mol Sci 2022, 23(16).
34. Micheau O, Tschopp J. Induction of TNF receptor I-mediated apoptosis via two sequential signaling complexes. Cell. 2003;114(2):181–90.
35. Rodríguez M, Cabal-Hierro L, Carcedo MT, Iglesias JM, Artime N, Darnay BG, Lazo PS. NF-kappaB signal triggering and termination by tumor necrosis factor receptor 2. J Biol Chem. 2011;286(26):22814–24.
36. Janssen HL, Higuchi H, Abdulkarim A, Gores GJ. Hepatitis B virus enhances tumor necrosis factor-related apoptosis-inducing ligand (TRAIL) cytotoxicity by increasing TRAIL-R1/death receptor 4 expression. J Hepatol. 2003;39(3):414–20.
37. Zhou X, Jiang W, Liu Z, Liu S, Liang X. Virus infection and death Receptor-Mediated apoptosis. Viruses 2017, 9(11).
38. Benedict CA. Viruses and the TNF-related cytokines, an evolving battle. Cytokine Growth Factor Rev. 2003;14(3–4):349–57.

39. Rastelli J, Hömig-Hölzel C, Seagal J, Müller W, Hermann AC, Rajewsky K, Zimber-Strobl U. LMP1 signaling can replace CD40 signaling in B cells in vivo and has unique features of inducing class-switch recombination to IgG1. Blood. 2008;111(3):1448–55.
40. Gupta S, Termini JM, Niu L, Kanagavelu SK, Schmidtmayerova H, Snarsky V, Kornbluth RS, Stone GW. EBV LMP1, a viral mimic of CD40, activates dendritic cells and functions as a molecular adjuvant when incorporated into an HIV vaccine. J Leukoc Biol. 2011;90(2):389–98.
41. Tamura K, Stecher G, Kumar S. MEGA11: molecular evolutionary genetics analysis version 11. Mol Biol Evol. 2021;38(7):3022–7.
42. Chen C, Wu Y, Li J, Wang X, Zeng Z, Xu J, Liu Y, Feng J, Chen H, He Y, Xia R. TBtools-II: A one for all, all for one bioinformatics platform for biological big-data mining. Mol Plant. 2023;16(11):1733–42.
43. Wang D, Zhang Y, Zhang Z, Zhu J, Yu J. KaKs_Calculator 2.0: a toolkit incorporating gamma-series methods and sliding window strategies. Genomics Proteom Bioinf. 2010;8(1):77–80.
44. Yang S, Wang Y, Mei K, Zhang S, Sun X, Ren F, Liu S, Yang Z, Wang X, Qin Z, Chang Z. Tumor necrosis factor receptor 2 (TNFR2)-interleukin-17 receptor D (IL-17RD) heteromerization reveals a novel mechanism for NF-κB activation. J Biol Chem. 2015;290(2):861–71.
45. Matsuzawa Y, Oshima S, Takahara M, Maeyashiki C, Nemoto Y, Kobayashi M, Nibe Y, Nozaki K, Nagaishi T, Okamoto R, et al. TNFAIP3 promotes survival of CD4 T cells by restricting MTOR and promoting autophagy. Autophagy. 2015;11(7):1052–62.
46. Fan Y, Ye MS, Zhang JY, Xu L, Yu DD, Gu TL, Yao YL, Chen JQ, Lv LB, Zheng P, et al. Chromosomal level assembly and population sequencing of the Chinese tree shrew genome. Zoological Res. 2019;40(6):506–21.
47. Xu L, Yu D, Fan Y, Peng L, Wu Y, Yao YG. Loss of RIG-I leads to a functional replacement with MDA5 in the Chinese tree shrew. Proc Natl Acad Sci USA. 2016;113(39):10950–5.
48. Yu D, Wu Y, Xu L, Fan Y, Peng L, Xu M, Yao YG. Identification and characterization of toll-like receptors (TLRs) in the Chinese tree shrew (Tupaia belangeri chinensis). Dev Comp Immunol. 2016;60:127–38.
49. Han Y, Sun X, Kuang D, Tong P, Lu C, Wang W, Li N, Chen Y, Wang X, Dai J, Zhang H. Characterization of tree shrew (Tupaia belangeri) interleukin-6 and its expression pattern in response to exogenous challenge. Int J Mol Med. 2017;40(6):1679–90.
50. Yu D, Xu L, Liu XH, Fan Y, Lü LB, Yao YG. Diverse interleukin-7 mRNA transcripts in Chinese tree shrew (Tupaia belangeri chinensis). PLoS ONE. 2014;9(6):e99859.
51. Yao YL, Yu D, Xu L, Fan Y, Wu Y, Gu T, Chen J, Lv LB, Yao YG. Molecular characterization of the 2',5'-oligoadenylate synthetase family in the Chinese tree shrew (Tupaia belangeri chinensis). Cytokine. 2019;114:106–14.
52. Wiens GD, Glenney GW. Origin and evolution of TNF and TNF receptor superfamilies. Dev Comp Immunol. 2011;35(12):1324–35.
53. Igaki T, Miura M. The Drosophila TNF ortholog Eiger: emerging physiological roles and evolution of the TNF system. Semin Immunol. 2014;26(3):267–74.
54. Hu S, Tamada K, Ni J, Vincenz C, Chen L. Characterization of TNFRSF19, a novel member of the tumor necrosis factor receptor superfamily. Genomics. 1999;62(1):103–7.
55. Shao Z, Browning JL, Lee X, Scott ML, Shulga-Morskaya S, Allaire N, Thill G, Levesque M, Sah D, McCoy JM, et al. TAJ/TROY, an orphan TNF receptor family member, binds Nogo-66 receptor 1 and regulates axonal regeneration. Neuron. 2005;45(3):353–9.
56. Vandenabeele P, Declercq W, Van Herreweghe F, Vanden Berghe T. The role of the kinases RIP1 and RIP3 in TNF-induced necrosis. Sci Signal. 2010;3(115):re4.
57. Shui JW, Kronenberg M. HVEM is a TNF receptor with multiple regulatory roles in the mucosal immune system. Immune Netw. 2014;14(2):67–72.

Publisher's note